JACS
JOURNAL OF THE AMERICAN CHEMICAL SOCIETY

Communication

pubs.acs.org/JACS

Quantification of Topological Coupling between DNA Superhelicity and G-quadruplex Formation

Sangeetha Selvam, Deepak Koirala, Zhongbo Yu, and Hanbin Mao*

Department of Chemistry and Biochemistry, Kent State University, Kent, Ohio 44242, United States

Supporting Information

ABSTRACT: It has been proposed that new transcription modulations can be achieved via topological coupling between duplex DNA and DNA secondary structures, such as G-quadruplexes, in gene promoters through superhelicity effects. Limited by available methodologies, however, such a coupling has not been quantified directly. In this work, using novel magneto-optical tweezers that combine the nanometer resolution of optical tweezers and the easy manipulation of magnetic tweezers, we found that the flexibility of DNA increases with positive superhelicity (σ). More interestingly, we found that the population of G-quadruplex increases linearly from 2.4% at σ = 0.1 to 12% at σ = −0.03. The population then rapidly increases to a plateau of 23% at σ < −0.05. The rapid increase coincides with the melting of double-stranded DNA, suggesting that G-quadruplex formation is correlated with DNA melting. Our results provide evidence for topology-mediated transcription modulation at the molecular level. We anticipate that these high-resolution magneto-optical tweezers will be instrumental in studying the interplay between the topology and activity of biological macromolecules from a mechanochemical perspective.

Consisting of a stack of tetrameric guanine (G) residues arranged in quadrilateral planes, DNA G-quadruplexes (Figure 1A, top inset) have been found in single-stranded telomeres and double-stranded gene promoters in human cells.[1] Since 2002, many biological functions of G-quadruplexes, transcription regulations in particular, have been documented.[2] A new transcription control mechanism can be achieved through the topological coupling between duplex DNA and G-quadruplexes.[3] This mechanism exploits the different folding kinetics and thermodynamic stabilities of G-quadruplexes and duplex DNA under superhelical constraints that evolve dynamically[4] during transcription elongation. In the wake of a transcription bubble, the negative template superhelicity[4,5] is expected to reduce the annealing rate of destabilized duplex DNA, while the G-quadruplex may be less affected. This can shift the population equilibrium toward G-quadruplexes, which have shown inhibitory effects on the transcription machinery.[2a] To test this new mechanism, it is necessary to introduce a DNA template whose superhelicity can be adjusted.

Natural plasmids in bacteria have superhelical densities, or superhelicities (σ), of −0.03 to −0.09.[6] To vary the superhelicity, either topoisomerase activity is controlled during plasmid preparation or DNA-intercalating ligands are applied to purified plasmids.[7,8] However, these methods often introduce dispersed superhelicity levels,[9] while application of ligands may alter the properties of the DNA duplex or G-quadruplex. These issues can be resolved by using magnetic tweezers,[10] in which a pair of magnets is employed to vary the superhelicities of individual torsionally constrained duplex DNA tethered to a magnetic bead.

In this work, we combined the nanometer resolution of dual-beam optical tweezers and the easy manipulation of magnetic tweezers into a new magneto-optical tweezers instrument [Figure 1A and Figure S1 in the Supporting Information (SI)]. With this instrument, we found that the flexibility of the DNA duplex increases with positive superhelicity. When a G-quadruplex-forming sequence in the insulin-linked polymorphic

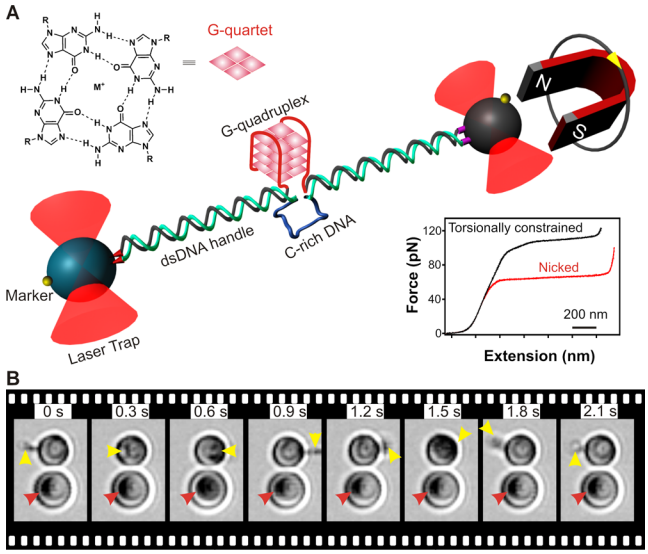

Figure 1. (A) Schematic of magneto-optical tweezers. A pair of rotary magnets is placed 20 mm above the two optically trapped beads. DNA is tethered between a streptavidin-coated magnetic bead (gray) (1.89 μm) and an antidigoxigenin-coated PS bead (blue) (2.1 μm). For clear observation, each bead is attached to a marker bead with a diameter of 130 nm. The top inset shows the structure of a G-quartet plane in a G-quadruplex. The bottom inset depicts a 120 pN plateau for torsionally constrained DNA (black) and a 65 pN plateau for nicked DNA (red). (B) Video frames of optically trapped beads during rotation of the magnets. With a torsionally constrained DNA tethered in between, only the magnetic bead (top) rotates while the PS bead remains still. Arrows depict the marker beads.

Received: June 26, 2014
Published: September 12, 2014

   dx.doi.org/10.1021/ja5064394 | J. Am. Chem. Soc. 2014, 136, 13967−13970

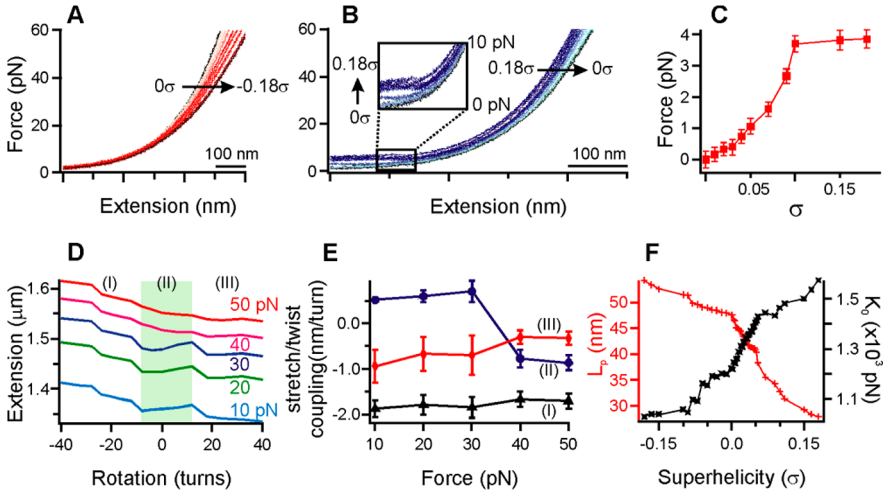

Figure 2. Mechanical properties of torsionally constrained λ-DNA. (A, B) Overlapped F–X traces at (A) negative and (B) positive superhelicities (σ) show that the extension at a given force decreases with σ. The inset in (B) shows that the low-force plateau increases with σ. (C) The transition force at the end of the plateau increases with σ until $\sigma = 0.1$. (D) DNA overwinding decreases the extension except at $\sigma = -0.02$ to 0.03 (region II) for $F < 40$ pN. (E) Except for region II, the stretch/twist coupling increases with force. (F) The persistence length (L_p) (red) decreases and the stretch modulus (K_0) (black) increases with σ.

region (ILPR) is incorporated into the λ DNA, we found that G-quadruplex formation increases with negative superhelicity. The start of the rapid increase in the G-quadruplex population coincides with the melting torque of the DNA duplex. In addition, neither the formation kinetics nor thermodynamic stability of the G-quadruplex varies with superhelicity. These results provide evidence that melting of the DNA duplex is required for folding of the G-quadruplex. As G-quadruplexes are known to modulate transcriptions, our results demonstrate the feasibility of transcription control through topological coupling between DNA duplexes and G-quadruplexes.

To prepare a torsionally constrained DNA duplex for superhelicity investigations, we modified two ends of a 4191 bp λ DNA with multiple copies of digoxigenin and biotin at both DNA strands (see Materials and Methods in the SI). We then attached the DNA construct between a digoxigenin-antibody-coated polystyrene (PS) bead (2.1 μm diameter) and a streptavidin-coated superparamagnetic bead (1.89 μm). These two beads were trapped by two 1064 nm laser foci separately.[11] To facilitate observation of the bead rotation, each bead was attached to a 130 nm diameter PS marker bead (Figure 1A).

The superhelicity of the DNA was controlled by a pair of magnets that rotated the superparamagnetic bead (Figure 1B). Since the PS bead was not perfectly spherical, rotation of the bead at the trapping focus in and out of the xy focal plane was prohibited because the electromagnetic field within the xz focal plane was anisotropic (Figure S4). In fact, the rotation of the PS bead was not observed even after 260 clockwise or anticlockwise revolutions of the magnetic bead at 0 pN of DNA tension, which introduced a σ of -0.65 to 0.65 to the λ DNA construct (see the SI for the calculation).

Next, we performed force-ramping experiments by moving the two beads apart while recording the tension in the DNA molecule in force–extension (F–X) curves (Figure 1A, bottom inset) in a 10 mM Tris buffer (pH 7.4) with 100 mM K^+ at room temperature. The torsionally constrained DNA construct was verified by the 120 pN plateau,[12] whereas the single-molecule nature was confirmed by single-rupture events observed during tether breakage (Figure 1A inset and Figure S6A). For the magnets that were 20 mm above the trapped beads, interference with the optical force measurement by the magnets was negligible, as the melting plateaus with and without magnets could be overlapped well (Figure S7B; the forces at which melting started[13] were 60.2 ± 1 pN with magnets and 61.1 ± 1 pN without magnets). The thermal effect of the magnetic beads in the laser trap was maintained at a negligible level of ~1 °C per 100 mW of laser power (Figure S2).

Close inspection of the F–X curves of the λ DNA revealed that unfolding events are rare. This is consistent with the absence of non-B DNA-forming sequences in the construct (see the SI). The overlap of the F–X curves for $\sigma = 0.18$ to -0.18 exhibited chiral behavior[10a,14] of the λ DNA (Figure 2). An increase in the low-force plateau (0 → 4 pN) became obvious only for $\sigma > 0.04$ (Figure 2B,C). These plateaus likely represent the formation or disassembly of plectonemes,[15] which occur more easily at positive superhelicities.[16] For $\sigma > 0.10$, the plateau force remained constant, probably reflecting saturation of the plectoneme formation in the construct. Except in the σ range from -0.02 to 0.03 for $F < 40$ pN (region II in Figure 2D), where positive stretch/twist coupling (0.42 nm/turn) leads to anomalous elongation of the extension with superhelicity,[16,17] shortening of the extension was observed when DNA was overwound. Such an observation quantitatively agrees with the literature.[15a,b] In addition, the high-resolution instrument directly verified the prediction[16] that the stretch/twist modulus (D), which is negatively proportional to the stretch/twist coupling constant (Figure 2E), decreases with force. Consistent with the literature,[10b,14b] the chiral bending property of double-stranded DNA (dsDNA) was also observed in twisting experiments performed at different forces (Figure S13).

To further quantify the mechanical properties of supercoiled DNA, we resorted to the Nelson model,[18] in which a dsDNA is considered as an isotropic rod whose energy is contributed by bending, stretching, twisting, and stretch/twist coupling (eq 2 in the SI). Given the small stretch/twisting coupling that does not vary with force significantly (Figure 2E), this model can be approximated by an extensible wormlike chain (WLC)[19] model (eq 3 in the SI) that accounts for the bending and stretching energies at a certain superhelicity level.[18] Indeed, comparison of the extensible WLC with a more comprehensive model that

dx.doi.org/10.1021/ja5064394 | J. Am. Chem. Soc. 2014, 136, 13967–13970

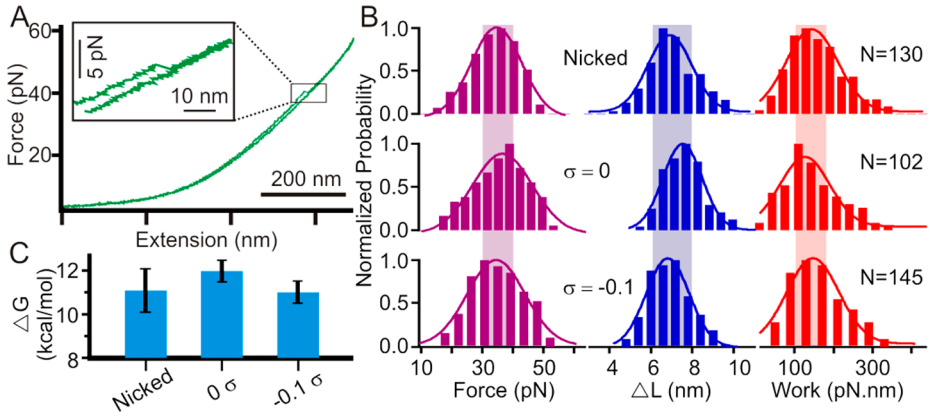

Figure 3. Mechanical unfolding of ILPR G-quadruplexes. (A) Typical F–X curve with an unfolding feature (inset) observed in 10 mM Tris buffer (pH 7.4) with 100 mM K^+. (B) Histograms of rupture force (purple), ΔL (blue), and unfolding work (red) for nicked (top) and torsionally constrained DNA at $\sigma = 0$ (middle) and −0.01 (bottom). Curves are Gaussian fits. (C) Changes in the unfolding free energy of ILPR G-quadruplex [$\Delta G_{unfold} \pm$ SD (bias); see the SI] do not vary with σ [11 ± 1 (−0.4), 12.0 ± 0.5 (0.03), and 11.0 ± 0.5 (0.2) kcal/mol for nicked, $\sigma = 0$, and −0.1 templates, respectively].

considers twist compliance of the dsDNA revealed similar fitting parameters for torsionally constrained dsDNA.[20] Here we fit F–X curves with this extensible WLC model to compare qualitatively the trends in persistence length (L_p) and stretch modulus (K_0) with σ (Figure S9). For σ = 0.18 to −0.18, the curves could be fit well between the plectoneme plateau and 43 pN, which represents the same force range used in the literature to interrogate the elastic properties of torsionally constrained DNA.[20] The fitting revealed that L_p decreases with σ while K_0 shows the reverse trend (Table S1 and Figure 2F). We reasoned that as σ increases, the DNA is more overwound, which leads to increased K_0 because the DNA is more difficult to stretch. While the L_p values fall within the range obtained from the same λ DNA,[10a] they are larger than those of the plasmids.[20] This may be ascribed to the non-B DNA structures formed in the plasmids. It is interesting that L_p decreases with σ, indicating that DNA bends more flexibly with increasing σ. Since plectonemes with increased flexibility[14a] nucleate more easily with positive superhelicity,[15a] the decrease in L_p may be caused by these sites. A similar trend in rotational flexibility was observed in fluorescence anisotropy experiments.[21] As positive superhelicity accumulates in front of a transcription bubble, the combined effects of increased flexibility and plectoneme formation may bring distal DNA and associated proteins closer to the transcription machinery in a head-on confrontation for potential transcriptional regulation.

To evaluate the effect of superhelicity on G-quadruplex formation, we incorporated an ILPR sequence, 5′-d-$(ACAGGGGTGTGGGG)_2$, into the λ DNA construct (see the SI) and mechanically stretched the DNA to a maximum force of 80 pN in the same buffer at pH 7.4. To ensure minimal force-induced DNA melting, we rotated the magnetic beads at 0 pN followed by incubation for 2 min. At $\sigma = 0$ (Figure 3A,B), we observed unfolding events with a change in contour length (ΔL) of ∼7 nm (see Figure S5 for the calculation), a value expected for the unfolding of the ILPR G-quadruplex or i-motif in the dsDNA context.[22] Since very few i-motifs form at pH 7.4,[23] the observed features are likely ILPR G-quadruplexes. The change in the free energy of unfolding (ΔG_{unfold}) calculated using the Jarzynski theorem[24] (eq 5 in the SI) was consistent with the ILPR G-quadruplex (∼11 kcal/mol).[22] Interestingly, the ΔG_{unfold} values for structures with $\sigma = 0$, $\sigma = -0.1$, or the nicked template were identical within experimental error (Figure 3C), indicating that the template superhelicity does not affect the thermodynamic stability of the G-quadruplex. However, since negative σ is expected to reduce the stability of the DNA duplex, the difference in ΔG_{unfold} for the G-quadruplex and dsDNA becomes larger with negative σ, which implies increased G-quadruplex population when σ becomes more negative.

To verify this implication, we unfolded structures in the ILPR–λ DNA construct in the physiologically relevant range of σ = −0.1 to 0.1.[6] We found structures of similar size ($\Delta L \approx 7$ nm) and mechanical stability ($F_{rupture} \approx 35$ pN) (Figure 4A and Figure

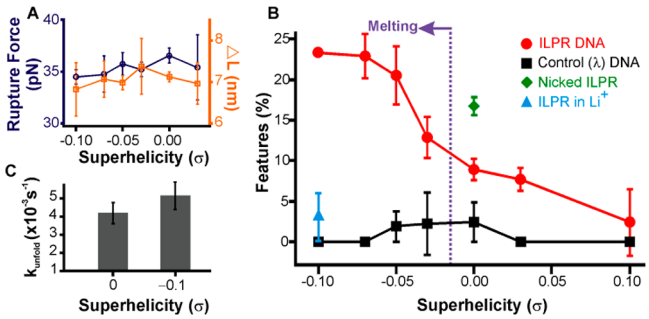

Figure 4. Topological coupling of G-quadruplex formation and DNA superhelicity. (A) Rupture force (violet) and ΔL (brown) show similar mechanical stabilities and sizes of ILPR G-quadruplex in DNA templates with σ = −0.1 to 0.03. (B) Percentage formation of folded structures vs template superhelicity in 10 mM Tris buffer (pH 7.4) with 100 mM K^+. Black: unfolding features observed in the λ construct that does not contain non-B DNA-forming sequences. Red: population of ILPR G-quadruplexes. Green: nicked DNA construct with ILPR G-quadruplex sequence. Blue: ILPR G-quadruplex in a σ = −0.1 template in 10 mM Tris buffer (pH 7.4) with 100 mM Li^+. See the SI for the calculation of the melting σ (−0.02 at τ = −10 pN nm).[15b,25,26] (C) Rate constants for G-quadruplex unfolding are similar within experimental error in DNA templates with $\sigma = 0$ (4.2×10^{-3} s^{-1}) and σ = −0.1 (5.2×10^{-3} s^{-1}).

S11) as those observed above for the G-quadruplex (also see ref 22). To confirm that these were G-quadruplex features, we performed experiments in the same Tris buffer but containing 100 mM Li^+ instead of K^+, which is known to inhibit ILPR G-quadruplex formation.[11] As expected, the population of folded structures in a σ = −0.1 template decreased from 23.3 to 3% (Figure 4B, blue).

The G-quadruplex population increases monotonically from 2.4% to 23.3% in the ILPR construct with decreasing σ (0.1 to

dx.doi.org/10.1021/ja5064394 | J. Am. Chem. Soc. 2014, 136, 13967−13970

−0.1) (Figure 4B). At $\sigma = 0.1$, the formation of the G-quadruplex is negligible compared with the λ DNA control construct, in which no folded structure is expected to form (Figure 4B, black squares). The population linearly increases with negative superhelicity until $\sigma \approx -0.03$ (Figure S12), which is followed by a rapid increase to a plateau of 23.3% at $\sigma < -0.05$. The superhelicity at which the rapid increase in G-quadruplex population takes place agrees rather well with the expected melting torque ($\sigma \approx -0.02$ at $\tau = -10$ pN nm),[15b,25,26] suggesting that DNA melting is required for G-quadruplex formation. The linear increase in the G-quadruplex population before the melting of dsDNA (Figure S12) suggests that the G-quadruplex may serve as a torque indicator. In the nicked DNA (green diamond in Figure 4B), a G-quadruplex population of 16% was observed, in agreement with a previous report.[22] This value is equivalent to that observed in the $\sigma \approx -0.04$ template, supporting the conclusion that local melting is required for G-quadruplex formation. According to the formula Lk = Tw + Wr,[27] where Lk is the link number, Tw is the physical twist between the two DNA strands, and Wr is the supercoiling along the dsDNA axis, nicks can release positive superhelical stress accumulated from localized melting by reducing Lk, which facilitates G-quadruplex formation. It is noteworthy that the saturated G-quadruplex formation (23.3%) matches the quadruplex population in single-stranded ILPR DNA (25%),[11] indicating that the complementary cytosine-rich strand does not interfere with the G-rich strand at $\sigma < -0.05$, which corroborates the requirement of DNA melting for G-quadruplex formation.

Analysis of the unfolding kinetics using the Dudko model[28] (see eq 7 in the SI) revealed similar k_{unfold} values at $F = 0$ pN (4−5 × 10^{-3} s^{-1}; see Figure 4C and Figure S14) among different superhelical densities. Since the values of ΔG_{unfold} are identical within experimental error (Figure 3C), this suggests that the G-quadruplex folding kinetics [calculated from the two-state model, $\Delta G_{unfold} \propto \ln(k_{unfold}/k_{fold})$] does not vary with template superhelicity. As the folding kinetics of the DNA duplex is expected to decrease with negative superhelicity, formation of the G-quadruplex is therefore kinetically favorable. With the thermodynamic difference between the G-quadruplex and duplex DNA observed above ($\Delta\Delta G_{unfold}$), we conclude that formation of the G-quadruplex is both kinetically and thermodynamically facilitated by negative superhelicities.

In summary, since the force and the bead-to-bead distance are measured by lasers in our magneto-optical tweezers, the superior temporal and spatial resolutions of optical tweezers are retained while the easy manipulation of magnetic tweezers is achieved. With this instrument, we found that the flexibility of DNA increases with positive superhelicity (σ). Since σ accumulates in front of a transcription bubble, this result suggests that distal DNA segments with associated proteins may encounter RNA polymerase head-on for possible modulations. In the wake of the transcription bubble, the topological coupling between G-quadruplex formation and negative DNA superhelicity provides justification for topology-based transcription control mechanisms at the molecular level.

■ ASSOCIATED CONTENT

Supporting Information

Methods and additional data. This material is available free of charge via the Internet at http://pubs.acs.org.

■ AUTHOR INFORMATION

Corresponding Author

hmao@kent.edu

Notes

The authors declare no competing financial interest.

■ ACKNOWLEDGMENTS

We are grateful to NSF (CHE-1026532) for financial support.

■ REFERENCES

(1) Biffi, G.; Tannahill, D.; McCafferty, J.; Balasubramanian, S. *Nat. Chem.* **2013**, *5*, 182.

(2) (a) Siddiqui-Jain, A.; Grand, C. L.; Bearss, D. J.; Hurley, L. H. *Proc. Natl. Acad. Sci. U.S.A.* **2002**, *99*, 11593. (b) Balasubramanian, S.; Hurley, L. H.; Neidle, S. *Nat. Rev. Drug Discovery* **2011**, *10*, 261. (c) Paeschke, K.; Bochman, M. L.; Garcia, P. D.; Cejka, P.; Friedman, K. L.; Kowalczykowski, S. C.; Zakian, V. A. *Nature* **2013**, *497*, 458.

(3) Sun, D.; Hurley, L. H. *J. Med. Chem.* **2009**, *52*, 2863.

(4) Kouzine, F.; Sanford, S.; Elisha-Feil, Z.; Levens, D. *Nat. Struct. Mol. Biol.* **2008**, *15*, 146.

(5) Wu, H.-Y.; Shyy, S.; Wang, J. C.; Liu, L. F. *Cell* **1988**, *53*, 433.

(6) Hatfield, G. W.; Benham, C. J. *Annu. Rev. Genet.* **2002**, *36*, 175.

(7) Keller, W. *Proc. Nat. Acad. Sci. U.S.A.* **1975**, *72*, 4876.

(8) Champoux, J. J. *Annu. Rev. Biochem.* **2001**, *70*, 369.

(9) Pulleyblank, D. E.; Shure, M.; Tang, D.; Vinograd, J.; Vosberg, H.-P. *Proc. Natl. Acad. Sci. U.S.A.* **1975**, *72*, 4280.

(10) (a) Strick, T. R.; Allemand, J.-F.; Bensimon, D.; Bensimon, A.; Croquette, V. *Science* **1996**, *271*, 1835. (b) Vilfan, I.; Lipfert, J.; Koster, D.; Lemay, S.; Dekker, N. In *Handbook of Single-Molecule Biophysics*; Hinterdorfer, P., Oijen, A., Eds.; Springer: New York, 2009; p 371. (c) Lebel, P.; Basu, A.; Oberstrass, F. C.; Tretter, E. M.; Bryant, Z. *Nat. Methods* **2014**, *11*, 456.

(11) Yu, Z.; Schonhoft, J. D.; Dhakal, S.; Bajracharya, R.; Hegde, R.; Basu, S.; Mao, H. *J. Am. Chem. Soc.* **2009**, *131*, 1876.

(12) Bustamante, C.; Bryant, Z.; Smith, S. B. *Nature* **2003**, *421*, 423.

(13) Zhang, X.; Chen, H.; Fu, H.; Doyle, P. S.; Yan, J. *Proc. Nat. Acad. Sci. U.S.A.* **2012**, *109*, 8103.

(14) (a) Marko, J. F. *Phys. Rev. E* **2007**, *76*, No. 021926. (b) Strick, T.; Allemand, J.-F.; Bensimon, D.; Croquette, V. *Biophys. J.* **1998**, *74*, 2016.

(15) (a) Van Loenhout, M.; de Grunt, M.; Dekker, C. *Science* **2012**, *338*, 94. (b) Forth, S.; Deufel, C.; Sheinin, M. Y.; Daniels, B.; Sethna, J. P.; Wang, M. D. *Phys. Rev. Lett.* **2008**, *100*, No. 148301. (c) Brutzer, H.; Luzzietti, N.; Klaue, D.; Seidel, R. *Biophys. J.* **2010**, *98*, 1267.

(16) Lionnet, T.; Joubaud, S.; Lavery, R.; Bensimon, D.; Croquette, V. *Phys. Rev. Lett.* **2006**, *96*, No. 178102.

(17) Gore, J.; Bryant, Z.; Nöllmann, M.; Le, M. U.; Cozzarelli, N. R.; Bustamante, C. *Nature* **2006**, *442*, 836.

(18) Nelson, P. C. *Biological Physics: Energy, Information, Life*, updated 1st ed.; W.H. Freeman: New York, 2008.

(19) Odijk, T. *Macromolecules* **1995**, *28*, 7016.

(20) Sheinin, M. Y.; Forth, S.; Marko, J. F.; Wang, M. D. *Phys. Rev. Lett.* **2011**, *107*, No. 108102.

(21) Selvin, P. R.; Cook, D. N.; Pon, N. G.; Bauer, W. R.; Klein, M. P.; Hearst, J. E. *Science* **1992**, *255*, 82.

(22) Dhakal, S.; Yu, Z.; Konik, R.; Cui, Y.; Koirala, D.; Mao, H. *Biophys. J.* **2012**, *102*, 2575.

(23) Dhakal, S.; Schonhoft, J. D.; Koirala, D.; Yu, Z.; Basu, S.; Mao, H. *J. Am. Chem. Soc.* **2010**, *132*, 8991.

(24) Jarzynski, C. *Phys. Rev. Lett.* **1997**, *78*, 2690.

(25) Liu, L. F.; Wang, J. C. *Proc. Natl. Acad. Sci. U.S.A.* **1987**, *84*, 7024.

(26) Bryant, Z.; Stone, M. D.; Gore, J.; Smith, S. B.; Cozzarelli, N. R.; Bustamante, C. *Nature* **2003**, *424*, 338.

(27) White, J. H. *Am. J. Math.* **1969**, *91*, 693.

(28) Dudko, O. K.; Hummer, G.; Szabo, A. *Proc. Natl. Acad. Sci. U.S.A.* **2008**, *105*, 15755.